Journal of the European Ceramic Society 38 (2018) 4245–4251

Contents lists available at ScienceDirect

Journal of the European Ceramic Society

journal homepage: www.elsevier.com/locate/jeurceramsoc

Original Article

Novel glass-ceramic SOFC sealants from glass powders and a reactive silicone binder

Hamada Elsayed[a,b], Hassan Javed[c], Antonio G. Sabato[c], Federico Smeacetto[d], Enrico Bernardo[a,*]

[a] Department of Industrial Engineering, Università degli Studi di Padova, Padova, Italy
[b] Ceramics Department, National Research Centre, Cairo, Egypt
[c] Department of Applied Science and Technology, Politecnico di Torino, Turin, Italy
[d] Department of Energy, Politecnico di Torino, Turin, Italy

ARTICLE INFO

Keywords:
Glass-ceramic sealant
XRD
Polymer-derived ceramics

ABSTRACT

The processing of sintered ceramics is often conditioned by the debinding step. The binders may determine some defects in the final product directly, by causing some gas evolution even at an advanced state of densification, due to incomplete decomposition at low temperature, or indirectly, by offering poor adhesion between particles, so that 'green' compacts may be easily damaged. The present investigation is aimed at exploring a novel concept for sintered glass-ceramics, based on the adoption of a silicone polymer as reacting binder, providing an abundant ceramic residue after firing. A glass belonging to the CaO-MgO-Al_2O_3-SiO_2 system, already studied as a sealant in solid oxide fuel cell (SOFC) planar stack design, was reproduced in form of 'silica-defective' variants, featuring a SiO_2 content, in the overall formulation, reduced up to 15 wt%. The overall silica content was recovered by mixing powders of the new glasses with the silicone: upon firing in air, the interaction between glass powders and polymer-derived silica led to glass-ceramics with the same phase assemblage than that formed by the reference glass and with a CTE of 9.5×10^{-6} K^{-1}. The new approach has been successfully applied to the manufacturing of glass-ceramic seals as joining materials for solid oxide cells.

1. Introduction

Glass-ceramics offer distinctive advantages in the manufacturing of solid oxide fuel cells (SOFCs) and solid oxide electrolysis cells (SOECs), when applied as sealants between the metallic interconnect (typically Cr-containing ferritic stainless steel) and the electrolyte (typically yttria stabilized zirconia) [1,2,3]. The chemical composition and the phase assemblage can be tailored in order to achieve a good thermo-mechanical and thermo-chemical compatibility with the joined materials. In particular, the coefficient of thermal expansion (CTE) must remain close to that of the surrounding materials, during thermal cycling [3], and self-healing effects, due to the presence of a remaining glassy phase, should be available [4].

Glass-ceramic sealants, like many other ceramic components obtained by sintering, are strongly conditioned by the debinding step. In fact, manual deposition or screen-printing rely on the use of fine glass powder particles mixed with organic binders (e.g. PVB [4]) in turn added with some solvent. Cracks and pores after firing, in any ceramic, may be due to gas evolution at high temperature, if the burn-out of organic matter is not completed at the early stages of heat treatment [5,6,7,8]. Less directly, and more specifically in the case of SOFC sandwich structures, the debinding may be critical for the handling in the 'green' state. Whereas substrates may be effectively glued together at room temperature, there is no actual binding in the interval between the temperature of complete burn-out of organic additives and the temperature required for significant viscous flow sintering to occur (the minimum temperature, in case of pressure less sintering, being represented by the dilatometric softening temperature) [9].

Among several compositions, we selected a previously studied glass belonging to the CaO-MgO-Al_2O_3-SiO_2 system, named V9, for the possibility to achieve a very good densification, by viscous flow sintering, with concurrent crystallization, at 850 °C. The compatibility between this sealant and pre-oxidised steel and the preservation of gas tightness (in dual atmosphere conditions) were demonstrated for a period of up to 1100 h. The main crystal phase, consisting Al-containing diopside ($CaMg_{0.7}Al_{0.6}Si_{1.7}O_6$), was found to be stable, except for some Al migration, favoring the precipitation of albite ($NaAlSi_3O_8$), upon long-term ageing [4].

The present paper is aimed at offering a novel strategy for the manufacturing of dense glass-ceramic sealants, by sintering (and concurrent crystallization) of fine glass powder particles, based on the adoption of a preceramic polymer as 'non-sacrificial' binder, not

* Corresponding author.
E-mail address: enrico.bernardo@unipd.it (E. Bernardo).

https://doi.org/10.1016/j.jeurceramsoc.2018.05.024
Received 2 January 2018; Received in revised form 14 May 2018; Accepted 18 May 2018
Available online 19 May 2018

subjected to complete burn-out, in analogy to what already done with advanced ceramics [10] or, more recently, with bioceramics from additive manufacturing [11]. Silicones represent a vast class of preceramic polymers, i.e. polymers providing an abundant ceramic residue after firing above 500–600 °C [12]; given the particular molecular structure, based on siloxanic chains, the ceramic residue may consists of amorphous silica or SiOC (silicon oxycarbide), depending on the firing atmosphere, oxidative or inert, respectively [12]. Owing to the transformation, silicones were reputed to bind glass particles even after their decomposition and keep sandwich structures joined up to high temperature; obviously, the presence of a ceramic residue had to be considered for its impact on the microstructure after firing.

Besides 'non-sacrificial', silicones actually configure 'reactive' binders. It is well known, in the field of polymer-derived ceramics, that the preceramic precursors are often used coupled with fillers, reacting with the transformation products (active fillers) or remaining inert (passive fillers) during firing [13,14]. In oxidative conditions, oxide fillers (represented directly by oxide powders, or by carbonates, hydroxides etc.) are known to combine easily with the silica residue from silicones, yielding a quite wide range of silicate ceramics [15]. Glass powders may be considered as additional oxide fillers, although their role is not strictly defined: glass may remain substantially inert, embedded in a polymer-derived matrix, as recently shown by Francis et al. [16], who explored silicone/bioglass coatings, subjected to thermal treatments at low temperature (not exceeding 500 °C), or 'integrate' in the final silicate ceramics [17,18,19].

Using a silicone resin as reactive binder represents an unprecedented case of integration between preceramic polymers and glass. The silica residue, in oxidative atmosphere, was intended to mix with glasses featuring an 'engineered' chemical composition, upon firing. In particular, glass-ceramics equivalent to those available from the above mentioned V9 glass were achieved by the interaction of the polymer-derived residues and fine powders of 'silica defective' glasses, as shown by the scheme in Fig.1. In other words, specific glass compositions were designed to 'absorb' the extra silica deriving from the same transformation. The effective integration and the successful replacement of V9-based glass-ceramics were demonstrated directly in new SOFC and SOEC joints.

2. Experimental procedure

Table 1 reports the chemical composition of the reference glass [4], named V9, and of two 'silica-defective' variants, V9′ and V9″, reproduced by decreasing the SiO_2 content in V9, but keeping the other oxides in the same relative proportions. V9 was produced by melting the raw materials (carbonates and oxides) in a furnace at 1600 °C for 1 h in a Pt-Rh crucible; the variants, due to the lower silica content, could be produced even at 1300 °C, for 1 h, in an alumina-silicate refractory crucible. The glasses were quenched by direct pouring on a cold metal plate. The glass fragments were easily reduced into fine powders by ball milling (considering the internal stresses determined by the sudden cooling) and later manually sieved; only the particles with a diameter below 75 μm were kept.

Table 1
Chemical composition and characteristic temperatures of the studied glasses.

	V9	Silica-defective glasses	
		V9'	V9''
Chemical composition (wt%)			
SiO_2	50.4	46.3	48.5
Al_2O_3	8.3	9.0	8.6
CaO	9.3	10.1	9.6
MgO	13	14.1	13.5
Na_2O	10.3	11.1	10.7
ZrO_2	2.9	3.1	3.0
B_2O_3	5.8	6.3	6.0
Characteristic temperatures (°C)			
Glass transition (T_g)	637	605	618
Dilatometric softening point	640	616	627
Littleton point	762	735	747
Reference	[4]	[21]	[21]

Monolithic pellets were prepared using glass particles, mixed with a commercially available methyl polysilsesquioxane resin ("silicone"), SILRES® MK (Wacker-Chemie GmbH, Munich, Germany). Solid MK was dissolved in isopropanol (15 ml for 10 g of final ceramic) and then mixed with glass powders. The mixing was performed under magnetic stirring, followed by sonication for 10 min, leading to stable and homogeneous dispersions. The mixtures were poured into large glass containers and dried at 80 °C overnight. After drying, the silicone-based mixtures were in the form of solid fragments, later converted into fine powders by ball milling at 350 rpm for 30 min. The powders were cold-pressed in a cylindrical steel die applying a pressure of 20 MPa for 1 min, without using any additive. Specimens having approximately

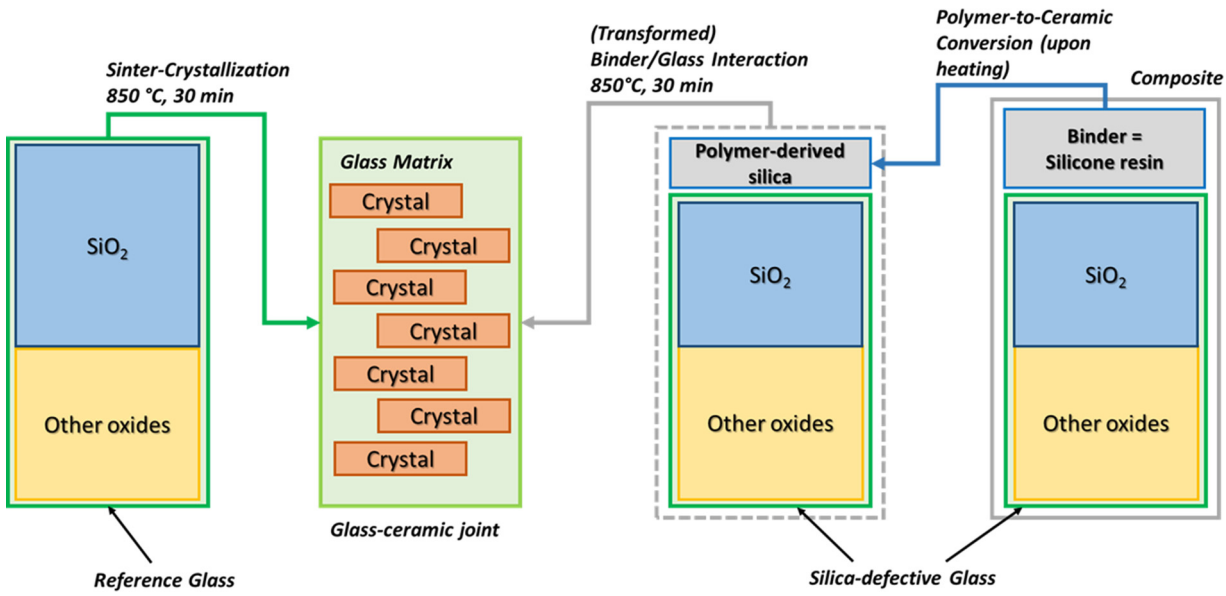

Fig. 1. Processing scheme for glass-ceramic joints: sinter-crystallization (left) compared with heat treatment of silicone/silica-defective glass mixtures (right).

Table 2
Formulations of the studied silicone/glass mixtures.

Batch		Components (g per 100 g product)				Oxide yields													
						SiO_2		Al_2O_3		CaO		MgO		Na_2O		ZrO_2		B_2O_3	
		MK	V9	V9′	V9″	(g)	%	(g)	%	(g)	%	(g)	%	(g)	%	(g)	%	(g)	%
A	*Binder*	8.9				7.5													
	Glass			91.1		42.2		8.2		9.2		12.8		10.1		2.8		5.7	
Total						49.7	**50.4**	8.2	**8.3**	9.2	**9.3**	12.8	**13.0**	10.1	**10.3**	2.8	**2.9**	5.7	**5.8**
B	*Binder*	4.5				3.8													
	Glass		50.0			25.2		4.1		4.6		6.5		5.1		1.4		2.9	
				45.5		21.1		4.1		4.6		6.4		5.1		1.4		2.9	
Total						50.1	**50.4**	8.2	**8.3**	9.2	**9.3**	12.9	**13.0**	10.1	**10.3**	2.8	**2.9**	5.8	**5.8**
C	*Binder*	4.5				3.8													
	Glass				95.5	46.3		8.2		9.2		12.9		10.2		2.9		5.7	
Total						50.1	**50.4**	8.2	**8.3**	9.2	**9.3**	12.9	**13.0**	10.2	**10.3**	2.9	**2.9**	5.7	**5.8**
Reference (V9)							**50.4**		**8.3**		**9.3**		**13.0**		**10.3**		**2.9**		**5.8**

17 mm in diameter and 3 mm in thickness were obtained. The adopted silicone-glass formulations, comprising V9, V9′ and V9″ glasses, are reported in Table 2. For comparison purposes, pellets from silicone-free glass powders were also prepared.

The pellets were fired by a two-step thermal treatment, in a muffle furnace. After a first step at 500 °C, for 2 h, dedicated to the polymer-to-ceramic conversion of MK, the maximum temperature was set at 850 °C, for 30 min. The heating rate was kept constant at 2 °C/min; natural cooling followed the second-high temperature step.

The pellets, after firing at 850 °C, were subjected to density determinations (by the Archimedes' method) and X-ray diffraction analysis (performed on powdered samples, by means of Bruker AXS D8 Advance, Karlsruhe, Germany). A semi-automatic phase identification was conducted by means of the Match! program package (Crystal Impact GbR, Bonn, Germany), supported by data from PDF-2 database (ICDD-International Centre for Diffraction Data, Newtown Square, PA). The microstructure of polished surfaces of pellets was analyzed also by scanning electron microscopy (SEM, FEI Quanta 200 ESEM, Eindhoven, Netherlands). Evaluations of the amount of residual porosity were performed by means of image analysis, performed by using the ImageJ program package [20], on micrographs from SEM.

Additional sintering studies were conducted by means of hot stage microscopy analysis (EM301, by Hesse Instruments, Osterode am Harz, Germany), with a heating rate of 5 K min^{-1}, on pellets of batches A, B and C. Glass particles mixed with commercially available silicone MK in different proportions (batch A, B, and C) were also analyzed by differential thermal analysis, DTA (Netzsch, Eos, Selb, Germany). DTA scans were recorded from room temperature up to 1250 °C with heating rate of 5 K min^{-1}.

The compatibility of "batch C" glass-ceramic with pre-oxidized Crofer22APU and 8YSZ electrolyte was analyzed and investigated also by SEM. Crofer22APU was pre-oxidized at 950 °C for 2 h. A homogenous slurry containing the "batch C" glass powder and isopropanol (70:30 wt%) was prepared and deposited manually to obtain Crofer22APU/Glass-ceramic/8YSZ joint. The green Crofer22APU/Glass/8YSZ joint was kept at room temperature for 12 h to evaporate the solvent. The joining was done according to the heat treatment mentioned above.

The coefficient of thermal expansion (CTE) different glass-ceramics was measured by using a dilatometer (Netzsch, DIL 402 PC/4) at a heating rate of 5 °C/min. The dilatometry was performed on the glass-ceramics samples with a diameter of 1 cm and height of 5 mm.

3. Results and discussion

The present investigation can be seen as an extension of the quite recent research on glass-ceramics, from glass-containing silicone-based mixtures. In general, the final microstructure can be widely tuned, operating with glass fillers crystallizing into phases that could be identical or not to those yielded by the interaction between silicone and other oxide fillers. Zocca et al. [11] as an example, described 3D-printed glass-ceramic scaffolds with apatite phase provided by the glass component and wollastonite mainly from the interaction between preceramic polymer and $CaCO_3$. Elsayed et al. [19], on the contrary, reported other scaffolds with crystal phases (wollastonite and diopside) provided both by silicone/fillers reaction and glass crystallization (with silicone/fillers mixtures and glass having the same overall chemical formulation). The glass filler is generally favorable, in polymer-derived silicate ceramics, in providing a liquid phase upon firing, enhancing the ionic interdiffusion and releasing the stresses developed during ceramization [17–19]. In the present case glass-ceramics were expected to form from silicone/glass mixtures in the absence of any other oxide filler, and the effectiveness of interactions had to be carefully assessed.

The first tests were conducted on samples from a silicone/V9′ glass mixture (batch A, Table 2). The formulation of V9′ had been carefully calculated in order to achieve, after its interaction with MK, the reference V9 composition. As reported in Table 2, the weight balance between components (8.9 g silicone mixed with 91.1 g V9′, for 100 g of mixture) was tuned on the particular polymer-to-ceramic conversion of MK. In fact, the silica residue (84% of the total weight of the polymer [15,19]; 8.9 g MK yielded about 7.5 g SiO_2) was expected to be added to the silica from V9′ glass. Compared to V9, V9′ had 15 wt% SiO_2 replaced by silica from MK (7.5 g in a total silica amount of 49.7 g, for 100 g of mixture A). The other oxides were obviously present only in the glass: more abundant in V9′, compared to V9, they were 'diluted' by the mixing of V9′ with the silica from MK. Table 2 reports data truncated to decimals, but the adopted MK/glass balance was actually calibrated for achieving, from batch A, the same overall oxide composition of the reference glass (V9).

X-ray diffraction analysis on samples after firing/sinter-crystallization treatment at 850 °C was carried out as a first tool for assessing any silicone/V9′ glass interaction. As shown by Fig.2a, there was a very good match in terms of the main crystal phase developed, between silicone/V9′ and the original glass. Al-containing diopside ($CaMg_{0.7}Al_{0.6}Si_{1.7}O_6$ [PDF#78-1392], corresponding to the replacement of Mg^{2+}-Si^{4+} couples, in the structure of pure diopside $CaMgSi_2O_6$, with two Al^{3+} ions), already found from V9 glass [4], was confirmed. Some extra peaks, marked by arrows in Fig.2a, however, could be observed.

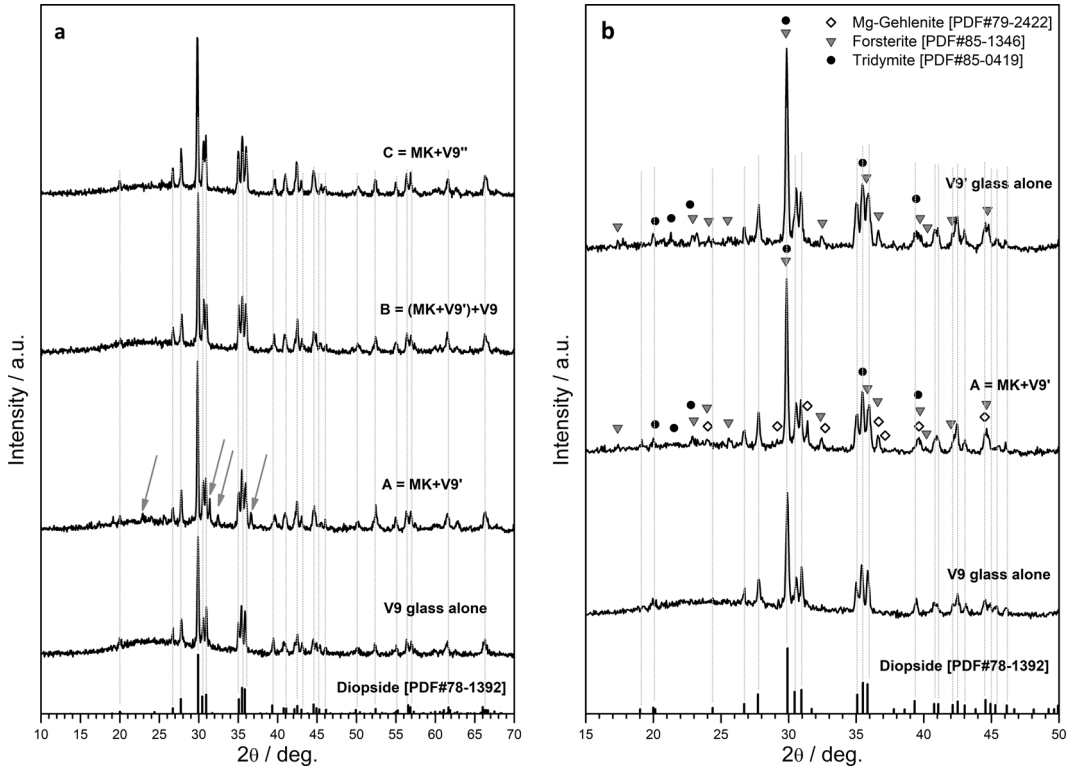

Fig. 2. Left: Comparison between glass-ceramics from different batches, all with the same overall chemical composition; right: comparison between glass-ceramics based on V9 and V9′ glasses.

In order to understand the origin of the extra peaks, we considered also a sample from the silica-defective V9′ glass, sinter-crystallized without 'composition compensation' from the MK polymer. As shown by Fig.2b, the extra peaks were partly due to the crystallization of V9′ and partly ascribed to the effective interactions between glass and ceramic residue of MK. In particular, forsterite (magnesium silicate, Mg_2SiO_4, PDF#85-1346) and tridymite (crystalline silica, PDF#85-0419) appeared in both glass-ceramics from batch A and from pure V9′, so that they could be considered as the product of the glass without any interaction with MK-derived silica. On the contrary, a gehlenite ($Ca_2Al_2SiO_7$)-akermanite ($Ca_2MgSi_2O_7$) solid solution (Mg-gehlenite, $CaMg_{0.25}Al_{1.5}Si_{1.25}O_7$, PDF#79-2422, according to the Match! Phase identification software), was found only in the glass-ceramic from batch A. Therefore, some interdiffusion between V9′ glass and ceramic residue of the silicone polymer could not be excluded, also considering the multitude of interfaces.

The interaction was further investigated by scanning electron microscopy (backscattered mode), as illustrated by Figs.3 and 4. In particular, from Fig.3b, we did not observe significant compositional gradients, that could be ascribed to MK-derived silica 'islands'. Crystal-free areas were visible in both silicone-free sinter-crystallized V9 (Fig.4a) and in the glass-ceramic from batch A. We can just observe a change in the distribution of crystals: the sinter-crystallization of V9 led to many tiny fibrous crystals, whereas batch A led to quite coarse 'bundles' of fibrous crystals.

Fig.3, in any case, shows a fundamental drawback of the proposed method: compared to glass-ceramic sample from V9, in Fig.3a, featuring limited isolated pores, that from batch A was much more porous. In particular, we can observe a number of pore clusters, attributed to gas release even in the high temperature stage. The substantial amount of residual porosity (in the order of 14 vol%, compared to 6% for V9 glass-ceramic) justifies the low density value shown in Fig.5.

Operating with batch A, the elimination of organic moieties from the silicone component, corresponding to the polymer-to-ceramic conversion, likely continued well above 500 °C, i.e. the temperature at which we originally planned an intermediate step in the heat treatment. A prolonged decomposition stage would be probably favorable, but another weakness can be envisaged. V9′, owing to the much reduced silica content, softened at much lower temperature than V9. As shown by Table 1, reporting data from SciGlass® database [21], V9′ had a transition temperature of only 605 °C, so that viscous flow sintering could actually overlap with the decomposition of MK; unreleased moieties could be 'trapped' by the pyroplastic mass determined by the same sintering of V9′.

Batch B was conceived in order to limit the drawbacks of the first application of the approach. More precisely, the amount of silica provided by MK was reduced to 7.5 wt% (3.8 g in a total silica amount of 50.1 g, for 100 g of mixture B), operating with a mix of V9′ and V9 glasses. Batch A was practically 'diluted' with V9 glass (batch B ideally consisted of a mixture of 50% batch A and 50% V9). The new formulation did not lead to any extra phase: as shown by Fig.2a, all diffraction peaks correspond to those of the reference silicate. Also in this case, some interdiffusion between glasses and MK-derived silica cannot be excluded, given the higher diffraction peaks, and lower background due to the amorphous phase, compared to sinter-crystallized V9′. The exact quantification will likely be the object of future investigations, but there was an undoubted promotion of crystallization, visible also from the quite dense (and homogenous) packing of crystals in Fig.4c.

The new formulation had a strong impact also on densification. Fig.3c shows that some relatively large pores remained, but the pore clusters, evidenced in the product of batch A, disappeared. The reduction of porosity (up to 10%) is testified by the density increase in Fig.5; although significant, however, the increase did not make samples from batch B comparable to the reference glass-ceramics. The presence of large pores could be attributed to the inherent inhomogeneity of the samples from batch B. The silica residue from MK interacted with glass particles with two different chemical compositions (V9 and V9′), so that

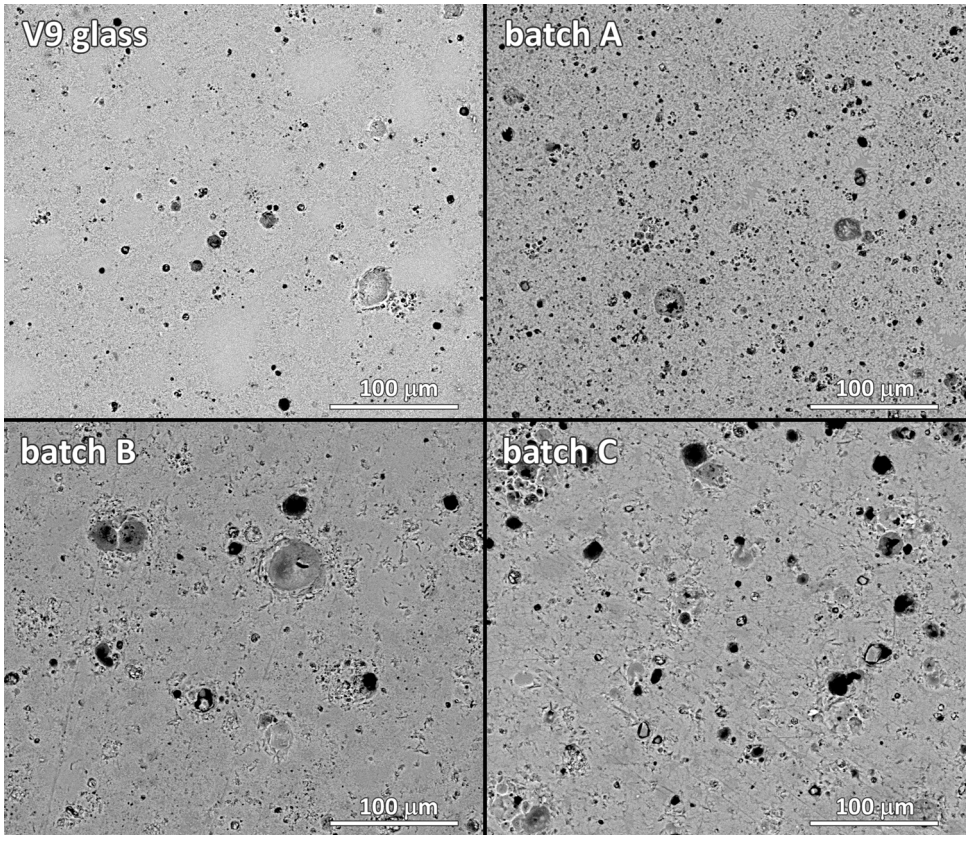

Fig. 3. Comparison of the polished cross-sections of glass-ceramics from different starting materials.

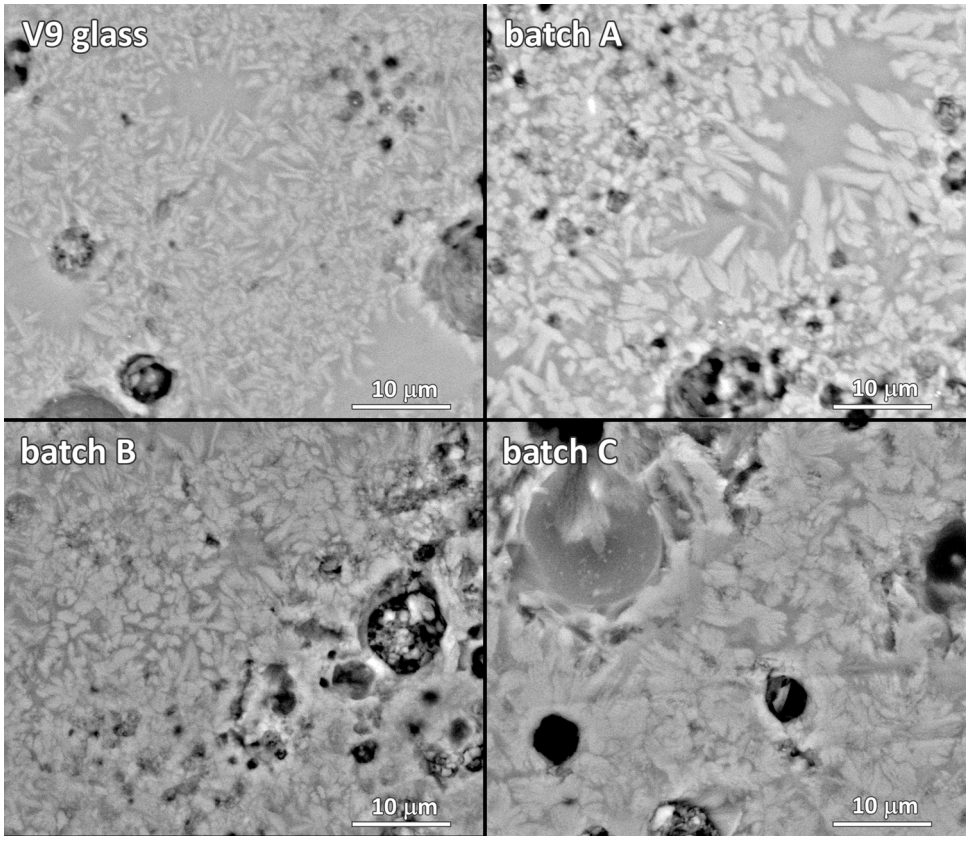

Fig. 4. High magnification details of the polished cross-sections of glass-ceramics from different starting materials.

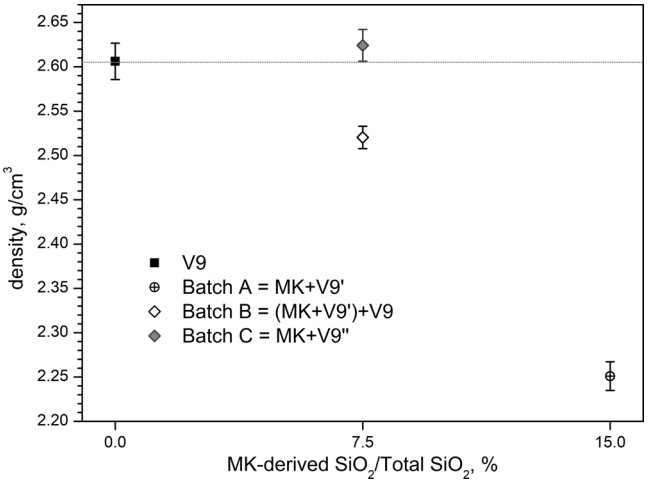

Fig. 5. Apparent densities of the developed glass-ceramics, as a function of the content of silicone MK.

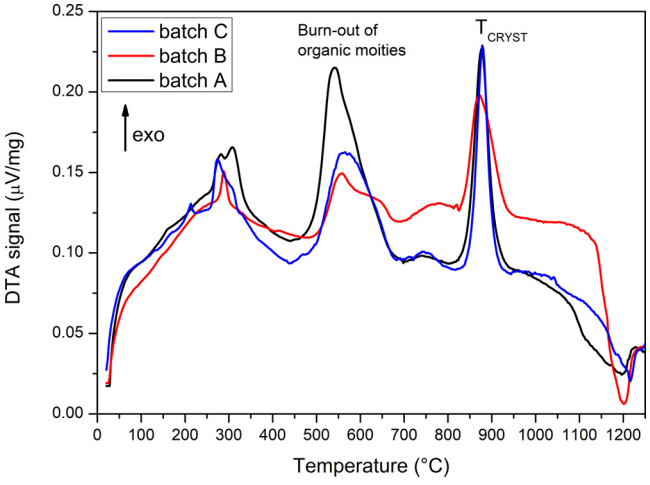

Fig. 7. DTA analysis on silicone-glass samples.

pore development could still be favored in low viscosity areas (from V9′).

With the purpose of keeping the reduced content of MK but increasing the overall homogeneity, owing to the use of only one glass component, we finally referred to batch C, based on V9″ glass. As shown by Table 2, V9″ had the same oxide yields than V9 and V9′ combined together, in batch B; given the higher silica content, compared to V9′, the softening could be appreciated at higher temperature (see the characteristic temperatures in Table 1). Also in this case, the match of crystal phase after firing could be confirmed, with no extra crystal phase (see Fig.2a); as expected, the porosity was more uniform (Fig.3d). Undoubtedly less abundant than in samples from A and B batches, the pores still remained quite numerous (8 vol%) compared to the reference glass-ceramic. The identity of density values (Fig.5) was likely caused by the enhanced density of the solid phase, in turn due to the above mentioned increase in crystallization (a multitude of crystal bundles can be observed also in Fig.4d).

Hot stage microscopy experiments, illustrated by Fig.6, were conducted in order to clarify the evolution of samples from different batches. Concerning batch A, a significant expansion behavior is visible above 800 °C. This trend is likely due to the interactions between glass and the ceramic residue of MK. The residual porosity, from gas release, could remain trapped as an effect of the viscosity increase caused by the crystallization of V9′. Concerning batches B and C, similar HSM curves were obtained; the expansion effect is less evident, at least at 850 °C, which was the joining temperature. Above 850 °C, interaction phenomena between glasses and MK-derived silica become also evident.

The DTA analysis, applied on glass/silicone mixtures, shown in Fig.7, is interesting in evidencing the more abundant release of moieties (exothermic peaks at 250–350 °C and 540–560 °C) from batch A, featuring the highest silicone content. The crystallization peak, as deduced by DTA analysis, was found to be at 875° ± 3 °C for all batches. On the basis of HSM and DTA plot, the sinter capability (difference between the temperature at which the maximum shrinkage occurs and the crystallization temperature), for all the three batches, is essentially similar and just slightly lower than that of the reference glass-ceramic [4].

The presence of pores in samples from batch C was not seen as a limitation for the application as sealing material in solid oxide fuel cell (SOFC) planar stack design. The thickness of glass-ceramic joints, in fact, is generally lower than the thickness of the produced pellets, so that the release of organic moieties was reputed to be favored. Furthermore, since all detected porosities are closed, they would likely not provide a gas path thus affecting the tightness. The latest product was even more attractive considering the dilatometric plots, shown in Fig.8. Despite the differences in crystallization, there was a good match in terms of coefficient of thermal expansion between the reference V9-derived glass-ceramic, already used as sealant, and the glass-ceramic from batch C. The latest sample featured a CTE of 9.6 × 10^{-6} K^{-1} (in the interval 200–500 °C), comparing favorably with that of the

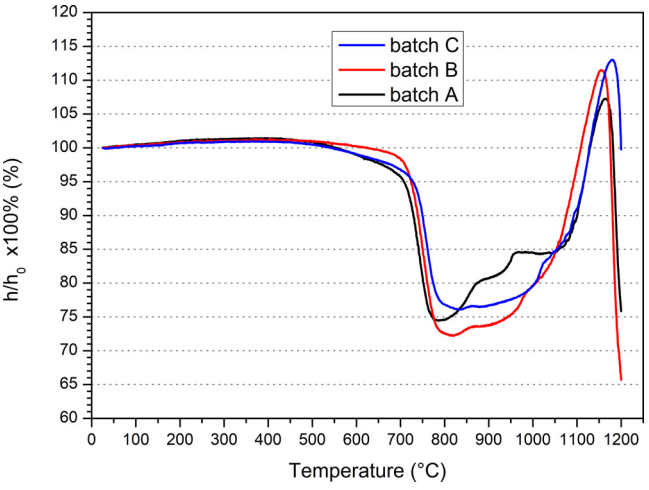

Fig. 6. Dilatometric densification curves (hot stage microscopy) for all batches.

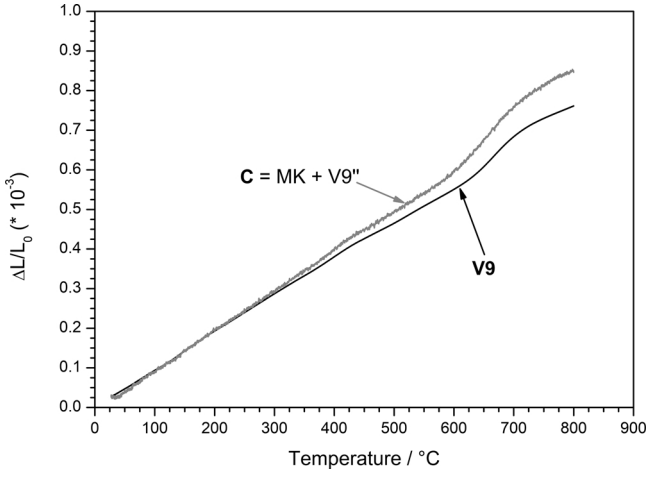

Fig. 8. Dilatometric plots for glass-ceramics derived from the sinter-crystallization of V9 glass and from the firing of batch C (MK + V9″ glass).

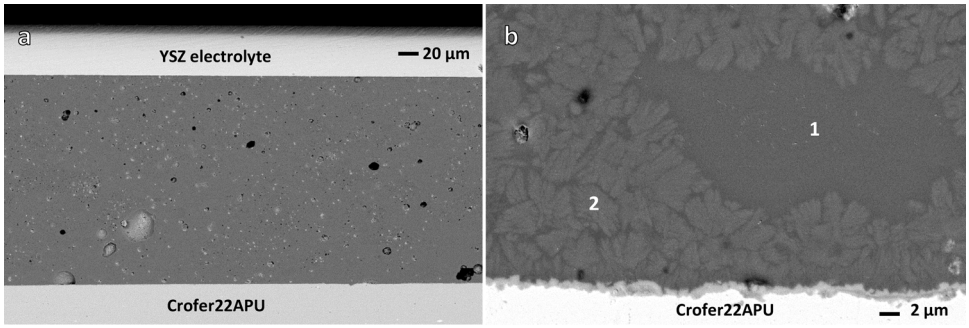

Fig. 9. Compatibility of "batch C" glass-ceramic with pre-oxidized Crofer22APU and 8YSZ.

reference (CTE = 9.52 10^{-6} K^{-1}) [4]. A residual glassy phase above 700 °C (see Fig.8) is also visible for both samples, as highlighted by the deviation from the linear behavior in the dilatometric curve, thus suggesting that residual amorphous phase could potentially provide a self-healing behavior.

Fig. 9a shows the compatibility of "batch C" glass-ceramic with pre-oxidized Crofer22APU and 3YSZ as investigated by SEM. SEM images showed a dense microstructure of the glass-ceramic and a good adhesion with both the Crofer22APU and the electrolyte. No delamination or cracks were observed at the interface between the glass-ceramic and the pre-oxidised Crofer22APU as well as at the glass-ceramic-electrolyte interface. Fig. 9b also shows significant residual glassy phase (zone 1) in addition to the crystalline phases (zone 2). The residual glassy phase is important to maintain the viscous behavior of the glass-ceramic and to increase the probability of self-healing, especially above glass transition temperature at the solid oxide cell device operating T (i. e. 800 °C). A thin layer of Cr_2O_3 (~1 µm), formed during the pre-oxidation of Crofer22APU, can be seen in Fig. 9b.

A final remark concerns the crystallization mechanism in the glass-ceramic from batch C. Diopside is known to undergo surface crystallization in glasses [22,23]. However, in presence of effective sintering by viscous flow before the crystals growth, the nuclei (formed on the surface of the glassy particles during the nucleation) can act as bulk nuclei during the growth. In our previous study [4], V9 glass-ceramic was found to crystallize by following this mechanism. Batch C is reputed be similar, although further investigations will be undoubtedly needed in order to clarify the contribution of internal interfaces represented by the boundaries between glass particles and the silica residue from the silicone matrix.

4. Conclusions

We may conclude that:

- Sintered glass-ceramics can be achieved by a novel method, i.e. by chemical interaction between a silicone resin and glass powders, inserted as fillers;
- With the same overall composition, the sinter-crystallization of a glass and the interaction between a silicone resin and 'silica-defective' variants of the same glass may lead to nearly identical phase assemblage;
- Silicone-glass mixtures can be exploited for the manufacturing of glass-ceramic seals as joining materials for solid oxide cells.

Acknowledgements

The research leading to these results has received funding from the European Union's Horizon 2020 research and innovation programme under the Marie Sklodowska-Curie grant agreement No. 642557 (CoACH – ETN: Advanced glasses, Composites And Ceramics for High growth Industries European Training Network). The authors thanks Ms Caterina Cesaroni (BSc student, University of Padova), for experimental assistance.

References

[1] N. Mahato, A. Banerjee, A. Gupta, S. Omar, K. Balani, Progress in material selection for solid oxide fuel cell technology: a review, Progr. Mat. Sci. 72 (2015) 141–337.
[2] N. Singh, Sealing technology for SOFCs, Int. J. Antimicrob. Agents 4 (2007) 134–144.
[3] J.W. Fergus, Sealants for solid oxide fuel cells, J. Power Sources 147 (2005) 46–57.
[4] A.G. Sabato, G. Cempura, D. Montinaro, A. Chrysanthou, M. Salvo, E. Bernardo, M. Secco, F. Smeacetto, Glass-ceramic sealant for solid oxide fuel cells application: characterization and performance in dual atmosphere, J. Power Sources 328 (2016) 262–270.
[5] J.R.G. Evans, M.J. Edirisinghe, J.K. Wright, J. Crank, On the removal of organic vehicle from moulded ceramic bodies, Proc. R. Soc. Lond. A 432 (1991) 321–340.
[6] M.J. Cima, J.A. Lewis, A.D. Devoe, Binder distribution in ceramic green ware during thermolysis, J. Am. Ceram. Soc. 72 (1989) 1192–1199.
[7] T. Chartier, M. Ferrato, J.-F. Baumard, Influence of the debinding method on the mechanical properties of plastic formed ceramics, J. Eur. Ceram. Soc. 15 (1995) 899–903.
[8] R.K. Enneti, S.J. Park, R.M. German, S.V. Atre, Review: thermal debinding process in particulate materials processing, mater, Manuf. Process. 27 (2012) 103–118.
[9] A. Ray, A.N. Tiwari, Compaction and sintering behaviour of glass-alumina composites, Mater. Chem. Phys. 67 (2001) 220–225.
[10] S.T. Schwab, C.R. Blanchard, R.C. Graef, The influence of preceramic binders on the microstructural development of silicon nitride, J. Mater. Sci. 29 (1994) 6320–6328.
[11] A. Zocca, H. Elsayed, E. Bernardo, C.M. Gomes, M.A. Lopez-Heredia, C. Knabe, P. Colombo, J. Günster, 3D-printed silicate porous bioceramics using a non-sacrificial preceramic polymer binder, Biofabrication 22 (7(2)) (2015) 025008.
[12] P. Colombo, G. Mera, R. Riedel, G.D. Soraru, Polymer-derived ceramics: 40 years of research and innovation in advanced ceramics, J. Am. Ceram. Soc. 93 (2010) 1805–1837.
[13] P. Greil, Active-filler-controlled pyrolysis of preceramic polymers, J. Am. Ceram. Soc. 78 (1995) 835–848.
[14] P. Greil, Polymer derived engineering ceramics, Adv. Eng. Mater. 6 (2000) 339–348.
[15] E. Bernardo, L. Fiocco, G. Parcianello, E. Storti, P. Colombo, Advanced ceramics from preceramic polymers modified at the nano-scale: a review, Materials 7 (2014) 1927–1956.
[16] A. Francis, R. Detsch, A.R. Boccaccini, Fabrication and cytotoxicity assessment of novel polysiloxane/bioactive glass films for biomedical applications, Ceram. Int. 42 (2016) 15442–15448.
[17] L. Fiocco, H. Elsayed, J.K.M.F. Daguano, V.O. Soares, E. Bernardo, Silicone resins mixed with active oxide fillers and Ca–Mg silicate glass as alternative/integrative precursors for wollastonite-diopside glass-ceramics foams, J. Non-Cryst. Solids 416 (2015) 44–49.
[18] M. Parchovianský, G. Barroso, I. Petríková, G. Motz, D. Galusková, D. Galusek, Polymer derived glass ceramic layers for corrosion protection of metals, ceramic for energy conversion, storage, and distribution systems, Ceram. Trans. 256 (2016) 187–200.
[19] H. Elsayed, P. Colombo, E. Bernardo, Direct ink writing of wollastonite-diopside glass-ceramic scaffolds from a silicone resin and engineered fillers, J. Eur. Ceram. Soc. 37 (2017) 4187–4195.
[20] W.S. Rasband, ImageJ, 1997–2011, U.S. National Institutes of Health, Bethesda, Maryland, USA, http://imagej.nih.gov/ij/.
[21] SciGlass, version 6.6 software (1998–2006), ITC Inc., Newton, MA, USA.
[22] A.G. Sabato, M. Salvo, A. De Miranda, F. Smeacetto, Crystallization behaviour of glass-ceramic sealant for solid oxide fuel cells, Mater. Lett. 141 (2015) 284–287.
[23] A.A. Francis, R.D. Rawlings, R. Sweeney, A.R. Boccaccini, Crystallization kinetic of glass particles prepared from a mixture of coal ash and soda-lime cullet glass, J. Non-Cryst. Solids 333 (2004) 187–193.